Climate and Cryosphere Cause Water Yield Regime Shifts in the Upper Brahmaputra River basin

Hao Li[1,2], Baoying Shan[3,2], Liu Liu[1], Lei Wang[4], Akash Koppa[2], Feng Zhong[5,2], Dongfeng Li[6], Xuanxuan Wang[1], Wenfeng Liu[1], Xiuping Li[4], and Zongxue Xu[7]

[1]Center for Agricultural Water Research in China, China Agricultural University, Beijing, China
[2]Hydro-Climate Extremes Lab, Ghent University, Ghent, Belgium
[3]Research Unit Knowledge-based Systems, Ghent University, Ghent, Belgium
[4]Institute of Tibetan Plateau Research, Chinese Academy of China, Beijing, China
[5]College of Hydrology and Water Resources, Hohai University, Nanjing, China
[6]Department of Geography, National University of Singapore, Singapore
[7]College of Water Sciences, Beijing Normal University, Beijing, China

Correspondence: Liu Liu (liuliu@cau.edu.cn)

Abstract. Although evidence of hydrological responses to climate is abundant, the reliable assessments of water yield (WY) over mountainous regions, such as the Upper Brahmaputra River (UBR) basin, remain unclear due to intensified cryospheric changes. Based on multi-station runoff observations, we examine long-term WY changes during 1982–2013 in the UBR basin, and find there are in general hydrological regime shifts in the late 1990s; magnitude increases in WY range from ∼10% to ∼80%, while its directions reverse from upward to downward after the late 1990s. Then, the double mass curve (DMC) technique is used to assess the effects of climate, vegetation, and cryosphere on WY changes. Results show that climate and cryosphere together contribute to over 80% of magnitude increases of WY in the entire UBR basin, in which the role of vegetation is nearly negligible. The combined effects, however, are either offsetting or additive, leading to slight or substantial magnitude increases, respectively. Climate change, particularly precipitation decrease leads to the downward WY trend in recent years, while melt waters under global warming may alleviate the water shortage in some basins. Therefore, the combined effects of climate and cryosphere on WY should be considered in future water resources management over mountainous basins, particularly involving co-benefits between upstream and downstream regions.

1 Introduction

Water yield (WY) in mountainous watersheds is crucial for sustaining fragile ecosystems in headwaters, supplying valuable freshwater resources to downstream lowlands, and balancing co-benefits between upstream and downstream areas, especially for large transboundary river systems (Viviroli et al., 2011). In mountainous watersheds, WY changes have been commonly, but separately, attributed to climate (Dierauer et al., 2018; Song et al., 2021), vegetation (Goulden and Bales, 2014; Zhou et al., 2021), and glaciers and snow melting (Huss and Hock, 2018; Biemans et al., 2019). These are expected to alter the spatial and temporal distribution of water resources (Tang et al., 2019) and further threaten water supply and food security downstream (Biemans et al., 2019). The Qinghai-Tibet Plateau (QTP, see Figure 1a), which is also known as "Asian Water Tower", supplies

water resources for major rivers in Asia, such as Brahmaputra, Salween, Mekong, Yangtze, Yellow, and Indus Rivers (Kang et al., 2010; Yao et al., 2010, 2019). As such, WY changes over this region significantly affect the use of water resources, prevention of natural disasters, and protection of aquatic functions for the livelihoods of approximately two billion people (Immerzeel et al., 2010). While, total river runoff has never been reliably assessed, and its responses to global warming remain unclear, despite some in-situ observations and runoff estimates from state-of-the-art remote sensing technology (Wang et al., 2021). Therefore, comprehensively assessing the impacts of climate, vegetation, and cryosphere on long-term WY changes, particularly magnitude and direction, is of great importance for the sustainable development of water resources in the QTP (Yao et al., 2019).

In recent years, changes in climate, vegetation, and cryosphere have affected WY in the QTP. For example, Fan and He (2015) highlighted the important role of precipitation in WY increases in the Salween and Mekong River basins. Li et al. (2020) found that elevated precipitation and cryosphere changes both contributed to substantial WY increases in the Tuotuo River basin. Similarly, Lutz et al. (2014) projected that increased precipitation near the Salween and Mekong Rivers and accelerated meltwater near the Indus River caused significant WY changes. Vegetation has also been proven to be vital for mountainous water resources; Li et al. (2017) showed that evaporation, mostly due to grassland restoration, decreased WY in the Yangtze River basin, while Li et al. (2021) suggested that vegetation greening may change the seasonality of water resources and increase WY during the dry season in the UBR basin.

Although a growing body of evidence has shown that WY is affected by climate, vegetation, and cryosphere in the QTP, most studies focus on individual basins, and also do not consider these three aspects together. As such, previous results may not fully reveal the spatial variabilities in WY. Of specific interest is the Upper Brahmaputra River (UBR, see Figure 1a) basin, which covers an area of over 198,636 km^2 and has large gradients in elevation, climate, and vegetation (Li et al., 2019b). Hence, it is imperative to provide a comprehensive, spatially differentiated study considering the effects of climate, vegetation, and cryosphere on WY changes in this region. However, studies of WY changes in the UBR basin are significantly hindered by the sparse network of hydrological observation stations (Li et al., 2019b; Wang et al., 2021; Yao et al., 2019), which leads to large uncertainties in river flow forecasts, and thus water resources assessments. Also, current precipitation estimates are highly uncertain owing to the complex topography of this region, which limits the ability to accurately model the relationships between precipitation and runoff (Sun and Su, 2020). Lastly, the present inadequate understanding of hydrological responses to complex interactions among climate, vegetation, and cryosphere limits the application of hydrological models in these mountainous watersheds (Pellicciotti et al., 2012). While, long-term observed runoff records and recent high-resolution precipitation datasets give a pathway for using statistical methods to estimate runoff responses to warming in the UBR basin.

Hence, this study here jointly assesses historical WY responses to climate warming and associated environmental changes in the UBR basin. To do this, we collect multi-station runoff observations and detect long-term WY changes during 1982–2013 in the UBR basin. And then, we use the double mass curve (DMC) to estimate the effects of climate, vegetation, and cryosphere on magnitude and direction changes in WY. This study is expected to provide essential information for water resources management in the UBR basin and other mountainous watersheds.

2 Data and Methods

2.1 Study area

The Brahmaputra River (known as the Yarlung Zangbo River, or YZR, in China), a transboundary river in the southern QTP, originates in the Gyama Langdzom Glacier and flows across China, India, and Bangladesh, before emptying into the Indian Ocean. The UBR basin is located above the Nuxia hydrological station (Figure 1a), and its river flow has significant implications on freshwater resources of South Asia. Here, we divide the UBR basin into the headstream (HYZR), upstream (UYZR), midstream (MYZR), downstream (LYZR), Nianchu River (NCR), and Lhasa River (LSR) basins by the locations of hydrological stations (Table 1 and Figure 1b).

The elevation gradient and the distance to the ocean in the UBR basin together contribute to a large spatial variability in climate (Sang et al., 2016). The annual precipitation in the HYZR basin is less than 400 mm, while that in the LYZR basin is nearly 1000 mm, and similarly, the annual actual evaporation increases gradually from upstream to downstream areas (Figure S1a+b). Meanwhile, water and energy availability modulate vegetation conditions (Li et al., 2019a); vegetation cover increases dramatically from the HYZR to the LYZR basin (Figure S1c). Additionally, cryospheric meltwater due to atmospheric warming has substantially altered hydrology conditions in this region (Cuo et al., 2019; Yao et al., 2010; Wang et al., 2021).

Table 1. Information of six basins divided by the locations of hydrological stations. The column "TP" indicates the turning point using the Pettitt method, in which a significant tuning point is labeled with *. Glaciers and snow area is acquired from the land use and cover in 2000 (see details in Dataset).

Abbrevation	Full names	Station	Total area (km^2)	Mean elevation (m)	Glaciers and snow percentage (%)	TP
HYZR	Headstream	Lhatse	49,739	5061	1.7	1995
UYZR	Upstream	Nugesha	43,916	4985	0.39	1998*
NCR	Nianchu River	Shigatse	14,359	4733	1.96	1997*
MYZR	Midstream	Yangcun	20,004	4681	1.81	1997*
LSR	Lhasa River	Lhasa	25,601	4879	0.72	1996
LYZR	Downstream	Nuxia	45,017	4586	2.51	1997

2.2 Dataset

Here we collect annual runoff observations from 1982 to 2013 and convert the river flow (m^3/s) into runoff depth (mm). Also, we acquire high-resolution climate and vegetation data in the same time range, and further aggregate these gridded data into regional annual values by considering area-weighted effects (their temporal changes are shown in Figure S2).

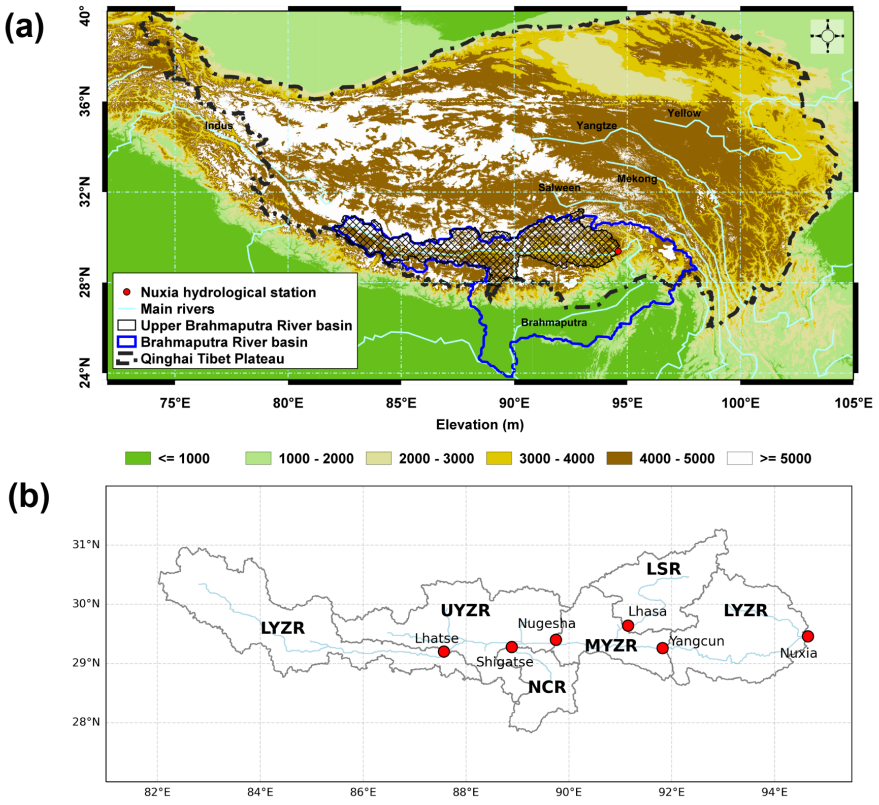

Figure 1. Location of (a) the Upper Brahmaputra River (UBR) basin in the Qinghai Tibet Plateau (QTP), which is from Li et al. (2021), and (b) six basins divided by Lhatse, Nugesha, Shigatse, Yangcun, Lhasa, and Nuxia hydrological stations.

2.2.1 Runoff data

Annual runoff data between 1982 and 2013 used here come from six hydrological stations along the mainstream and major branches in the UBR basin. WY in the HYZR is equal to runoff depth at Lhatse station, while WY in other basins is calculated by the difference between runoff depth from the downstream station and that from the upstream and branch stations. For example, WY in the MYZR basin is equal to the difference between runoff depth in Yangcun station and that in Lhasa and Nugesha stations (Figure 1b).

2.2.2 Climate data

The most recent 10x10 km gridded daily precipitation data, combining topographic and linear correction approaches based on 262 rain-gauge observations, is developed for the UBR basin by Sun and Su (2020) and here used to estimate regional annual precipitation (P). The maximum 2 m air temperature is obtained from China Meteorological Forcing Dataset (He et al., 2020). Regional actual evaporation (AET) with a 0.25° spatial resolution is acquired from Global Land Evaporation Amsterdam

Model (GLEAM) (Martens et al., 2017). The evaporation product has been validated in different biome types in China and shown high correlations with in-situ eddy covariance AET (Yang et al., 2017).

2.2.3 Vegetation data

The leaf area index (LAI) used in this study is obtained from Global Inventory Monitoring and Modelling System (GIMMS) LAI3g with a spatial resolution of 8×8 km (Zhu et al., 2013). The product is generated using an artificial neural network trained on the Collection Terra Moderate Resolution Imaging Spectroradiometer (MODIS) LAI product and the latest version of GIMMS NDVI3g data for the same period, which has been proven to have an improved multi-sensor record harmonization scheme compared to other global LAI products (Forzieri et al., 2020; Gonsamo et al., 2021).

2.2.4 Land use and cover

The land use and cover in 2000 with a spatial resolution of 1x1 km is used to represent the land cover types in the UBR basin. The data is acquired from Resource and Environmental Science Data Center, and is here divided into seven primary land use types, including cultivated land, forestland, grassland, water body, urban land, unused land, and glaciers and snow (Figure S3).

2.3 Methodology

2.3.1 Trend and abruption analysis

In this study, we use the non-parametric Mann–Kendall test (Kendall, 1938; Mann, 1945) to identify the trend in WY, and Pettitt abrupt detection (Pettitt, 1979) to identify the turning point (TP) in WY, where the level of significance is set at 0.05. We then compare the averages of WY before and after the TP to reflect the magnitude changes, and compare the trends in two periods to reflect the direction changes.

2.3.2 Double mass curve technique

The DMC used here is a plot of the cumulative data of one variable versus the cumulative data of another related variable in a concurrent period. It has previously been used to assess the individual effect of climate (Gao et al., 2011), forest disturbance (Wei and Zhang, 2010), wildfire (Hallema et al., 2018), and cryosphere (Brahney et al., 2017) on water resources. For the large and pristine UBR and other mountainous basins, climate, vegetation, and cryosphere (melt waters from glaciers and snow under warming, see Biemans et al. 2019; Huss and Hock 2018) play important roles in hydrology, and these three parts must be together considered to accurately estimate hydrological responses to warming. It is considerably hard to directly calculate the supply of melt waters to WY due to the lack of long-term glacier monitoring, while runoff observations and high-resolution climate and vegetation data make it possible to use the DMC technique, a data-driven statistical method, to estimate cryospheric contributions to WY.

The selection of climate and vegetation indices used in the DMC technique is an important issue. Previous studies have shown that effective precipitation (eP, P-AET) can reflect more information of climate on WY compared with individual P or

AET, and be regarded as a reliable proxy to climate (Wei and Zhang, 2010; Zhang et al., 2019). LAI quantifies the amount of leaf area in an ecosystem and becomes an important variable reflecting vegetation structures and biophysical processes (Fang et al., 2019; Forzieri et al., 2020), and Li et al. (2021) has used LAI to investigate vegetation effects on seasonal hydrology in the UBR basin. Hence, we consider eP and LAI as the indices of climate and vegetation respectively, and use their time series as the inputs in the DMC model.

To obtain cryospheric contributions to WY, we firstly build two types of DMC plots (see Figure S4) to assess the contributions of climate (eP) and vegetation (LAI), and then subtract the sum of estimated contributions from total WY deviations as cryospheric effects (results are shown in Figure S5). The schematic diagram Figure 2 and associated mathematical formulas are shown as follows:

First, the total WY deviation ($\Delta WY_s(t)$, black diamond in Figure 2c) can be calculated as the difference between WY after a TP ($WY_o(t)$, red point in Figure 2b) and the average WY before that TP ($\frac{\sum_{t=1}^{t=tp} WY_o(t)}{tp}$, horizontal black line in Figure 2b), as follows:

$$\Delta WY_s(t) = WY_o(t) - \frac{\sum_{t=1}^{t=tp} WY_o(t)}{tp}, t = tp+1, tp+2, \ldots, 32 \tag{1}$$

Second, the regression equation (left panel in Figure 2a) between the cumulative eP ($\sum eP$) and cumulative WY ($\sum WY$) before a TP can be constructed as follows:

$$\sum WY = a_1 \sum eP + b_1 \tag{2}$$

Similarly, the regression equation (right panel in Figure 2a) between the cumulative LAI ($\sum LAI$) and cumulative water yield ($\sum WY$) before a TP can be constructed as follows:

$$\sum WY = a_2 \sum LAI + b_2 \tag{3}$$

Third, WY driven by climate ($WY_c(t)$, blue line in Figure 2b) can be calculated by inputting the cumulative eP after a TP into Equation 2. Therefore, WY deviation caused by climate change ($\Delta WY_c(t)$, blue bar in Figure 2c) can be calculated as follows:

$$\Delta WY_c(t) = WY_c(t) - \frac{\sum_{t=1}^{t=tp} WY_o(t)}{tp}, t = tp+1, tp+2, \ldots, 32 \tag{4}$$

Similarly, WY driven by vegetation ($WY_v(t)$, tan line in Figure 2b) can be calculated via Equation 3, and WY deviation caused by vegetation (ΔWY_v, tan bar in Figure 2c) can be calculated as follows:

$$\Delta WY_v(t) = WY_v(t) - \frac{\sum_{t=1}^{t=tp} WY_o(t)}{tp}, t = tp+1, tp+2, \ldots, 32 \tag{5}$$

Finally, WY deviation caused by cryosphere (ΔWY_g, red bar in Figure 2c) can be calculated as:

$$\Delta WY_g(t) = \Delta WY_s(t) - \Delta WY_c(t) - \Delta WY_v(t) \tag{6}$$

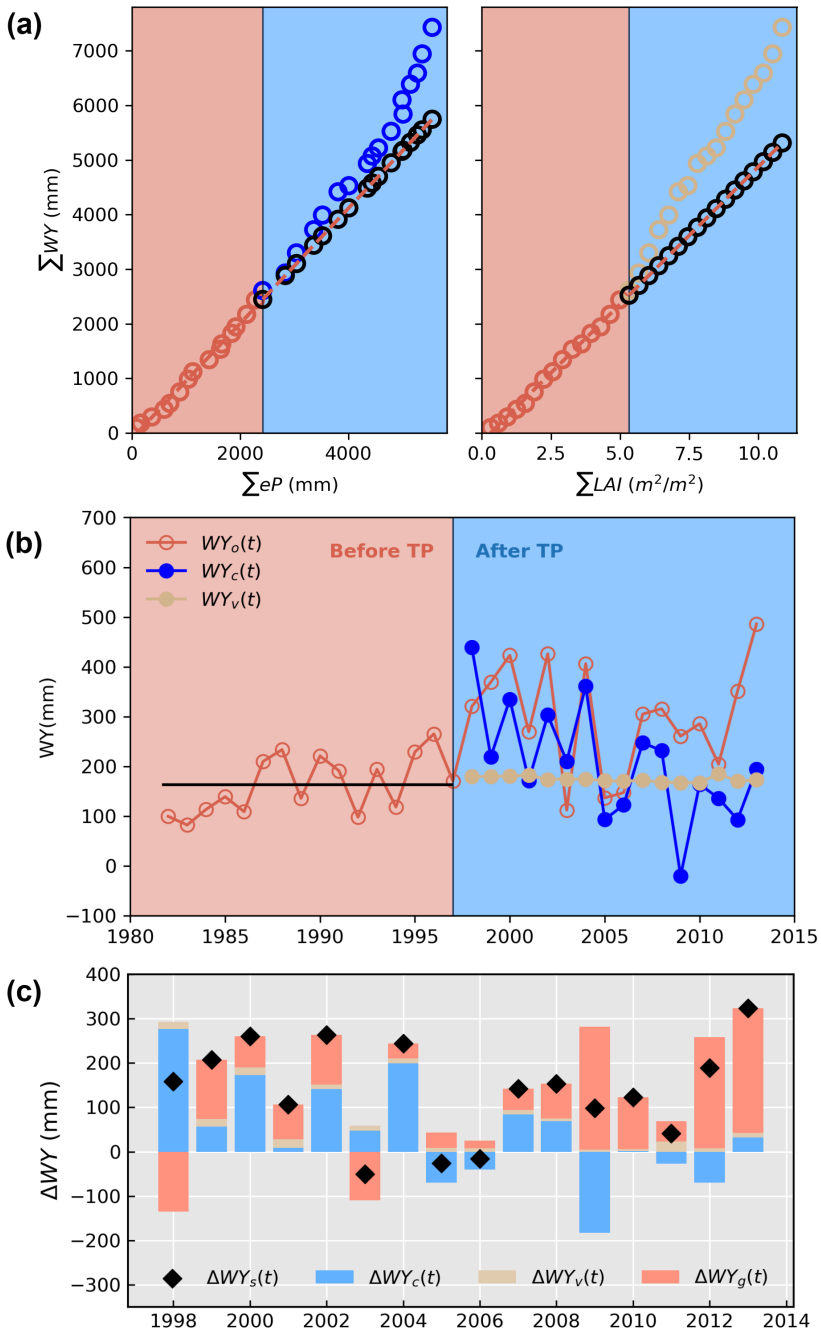

Figure 2. The schematic diagram showing how to estimate the effects of climate, vegetation, and cryosphere on water yield in the MYZR basin (see details in Methodology).

2.3.3 Attribution analysis on changes in water yield

The average contributions of climate, vegetation, and cryosphere to WY magnitude changes are calculated as follows:

$$\overline{\Delta WY_c} = \frac{\sum_{t=tp+1}^{t=32} WY_c(t)}{32-tp}$$
$$\overline{\Delta WY_v} = \frac{\sum_{t=tp+1}^{t=32} WY_v(t)}{32-tp}$$
$$\overline{\Delta WY_g} = \frac{\sum_{t=tp+1}^{t=32} WY_g(t)}{32-tp} \quad (7)$$

The relative contribution (RC), ranging from 0 to 1, of climate, vegetation, and cryosphere can be calculated as follows:

$$RC_c = \frac{|\overline{\Delta WY_c}|}{|\overline{\Delta WY_c}| + |\overline{\Delta WY_v}| + |\overline{\Delta WY_g}|}$$
$$RC_v = \frac{|\overline{\Delta WY_v}|}{|\overline{\Delta WY_c}| + |\overline{\Delta WY_v}| + |\overline{\Delta WY_g}|}$$
$$RC_g = \frac{|\overline{\Delta WY_g}|}{|\overline{\Delta WY_c}| + |\overline{\Delta WY_v}| + |\overline{\Delta WY_g}|} \quad (8)$$

Additionally, we use the Pearson correlation coefficient (r) to quantify the relationships between total WY deviation ($\Delta WY_s(t)$) and its components: WY deviation caused by climate ($\Delta WY_c(t)$), vegetation ($\Delta WY_v(t)$) and cryosphere ($\Delta WY_g(t)$). The Student's t-test is used to detect the statistical significance of the correlation coefficient at the level of 0.05.

3 Results

3.1 Long-term changes in historical water yield

The detection of long-term WY changes from 1982 to 2013 in the entire UBR basin is illustrated in Figure 3. There is a great spatial variability in WY (Figure 3a). The mean WY is the highest in the LYZR basin (over 600 mm), followed by that in the LSR basin (nearly 400 mm). However, the mean WY in the HYZR and NCR basins is less than 100 mm. This spatial variability is consistent with that of precipitation (Figure S6), which is mainly determined by elevation and distance to the ocean (Sang et al., 2016). In addition, WY generally increases during the period, as shown by the positive slope in Figure 3b, although the significant trend is only detected in the UYZR and MYZR basins (hatched areas in Figure 3b).

We then use the Pettitt method to identify the TP in WY. The TP mainly occurs during the late 1990s (Figure 3c), but the abrupt change detected in some basins is not statistically significant (Table 1). Similarly, the cumulative anomaly curve (Figure 3d) shows that WY decreases prior to the late 1990s and then increases in the entire UBR basin, which further supports the results obtained from the Pettitt method.

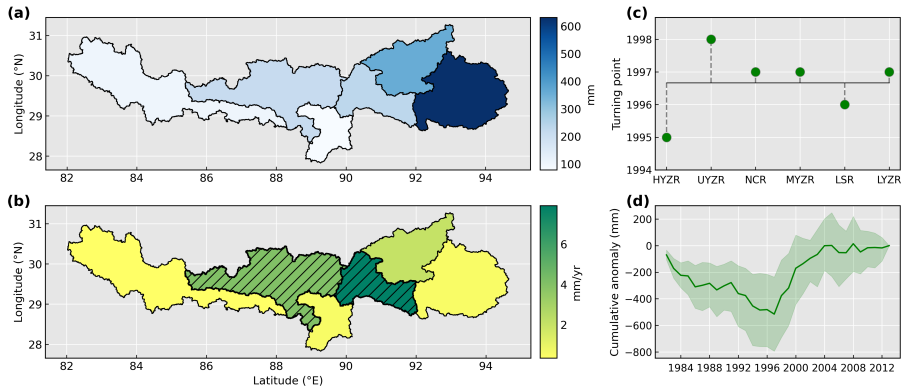

Figure 3. Long-term water yield changes in the six basins, covering the entire UBR basin. (a) The mean annual values by averaging water yield from 1982 to 2013. (b) The temporal trends detected by the Mann-Kendall Sen's slope method. The black hatching represents statistically significant ($p < 0.05$) trends. (c) The turning points (TP) detected by the Pettitt method. (d) The cumulative anomaly curve of water yield. The solid green line represents the ensemble expectation of cumulative anomaly curves of water yield for the entire UBR basin (green shading).

3.2 Regime shifts in historical water yield

Based on the TP, we divide the period from 1982 to 2013 into before and after TP periods, and analyze the magnitude and direction changes in WY in the entire UBR basin. Figure 4a shows that WY increases from 9.5 to 130.9 mm, with a high spatial variability. The slight increase observed in the HYZR and LYZR basins accounts for less than 10% of the mean WY before the TP, while a substantial WY increase of 61.6% and 80.5% is found in the UYZR and MYZR basins, respectively. In addition, a higher variation is detected after TP, suggesting a more dramatic variability in recent years.

For the direction changes in WY, we find that the trend is positive before the TP, but become negative afterward in most basins (Figure 4b and S2). The significantly decreasing trend is detected in the UYZR, NCR, and LSR basins. In contrast, although the WY in the MYZR basin increases during two periods, the rate has slowed, as the positive trend after the TP (3.64 mm yr^{-1}, $p > 0.05$) is less than that before the TP (8.95 mm yr^{-1}, $p < 0.05$). Overall, WY regime shifts occur in the late 1990s in the entire UBR basin; the magnitude generally increases, but the direction of WY has reversed or slowed.

3.3 Attribution analysis on magnitude increases in water yield

As shown in Figure 5, we quantify the contributions from climate (eP), vegetation (LAI), and cryosphere on WY magnitude increases in the entire UBR basin. We find that cryosphere changes, on average, contribute to over half of WY increases in the HYZR, UYZR, NCR, and MYZR basins. However, climate plays a more important role in WY magnitude increases in the LSR and LYZR basins, with average relative contributions of 55.4% and 46.0%, respectively. In contrast to the dominant roles of climate and cryosphere, vegetation has a consistently positive contribution to WY increases, although its relative contribution is much less than those from climate and cryosphere.

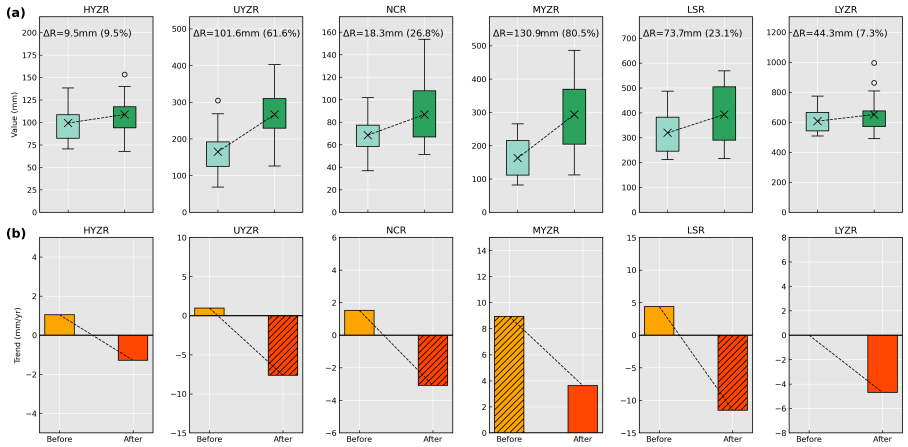

Figure 4. Water yield regime shifts in the entire UBR basin. (a) Magnitude of water yield changes. Black "x" signals show the mean of water yield in each boxplot. (b) Direction of water yield changes. The black hatching represents the statistically significant trend ($p < 0.05$). The color of boxes represents the period before (light color) and after (dark color) the turning point (TP).

Climate and cryosphere – two important factors affecting WY – together contribute to over 80% average magnitude increases of WY in the entire UBR basin; however, they play both additive or offsetting roles (Figure 5), resulting in slight or substantial WY increases (Figure 4a). For example, although cryospheric loss contributes to average increases of 28.3 mm and 30.3 mm in the HYZR and NCR basins (black "x" signals in Figure 5a+c), the negative contributions from climate offset a considerable part of these increases, leading to slight increases after the TP in these regions. Similarly, the positive contribution from climate offsets the negative contribution from cryosphere in the LSR and LYZR basins, which also results in a slight mean WY increase. In addition, the additive effects from climate and cryosphere lead to substantial increases in WY from 162.6 mm to 293.5 mm in the MYZR basin and from 164.9 mm to 266.5 mm in the UYZR basin (Figure 4a).

3.4 Attribution analysis on direction shifts in water yield

Pearson's correlation coefficient is applied to determine the role of climate, vegetation, and cryosphere in the reversed or slowed WY trend after the TP, as shown in Figure 4b. Results in Figure 6 show that, although the correlation varies greatly across basins ranging from 0.11 to 0.93 after the TP, climate typically is positively associated with total WY, in which the correlation is significant in half of basins ($p < 0.05$), again revealing the major role of climate in the hydrological trends in the entire UBR basin. Further analysis shows that, precipitation is much more important, because it exhibits the stronger reverse in trend compared with that in actual evaporation (Figure S7), which is also similar with direction changes in WY (Figure 4b). Additionally, despite the weak contribution of vegetation (Figure 5), its positive role in WY changes is more apparent in the drier basins (such as UYZR and NCR), while the correlation is negative in the relatively humid LYZR basin.

In contrast to positive contributions of climate, we find that WY caused by cryosphere exhibits a negative association with reduced total WY deviations in recent years in the UYZR ($r = -0.39$, $p > 0.05$) and LSR ($r = -0.36$, $p > 0.05$) basins. The negative

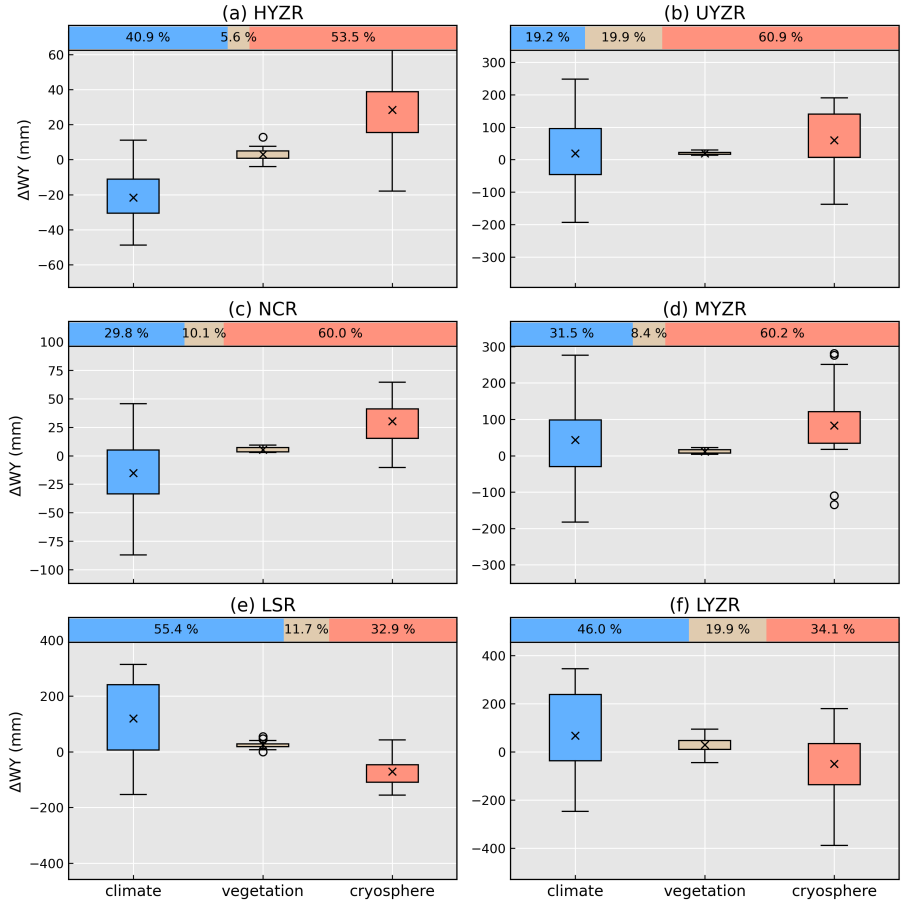

Figure 5. Attribution analysis of magnitude increases in water yield due to climate (ΔWY_c, blue box), vegetation (ΔWY_v, tan box), and cryosphere (ΔWY_g, red box), and their relative contributions (the bar with colors on the top) in each basin. Black "x" signals show the mean of water yield deviations (see Figure S5) in each boxplot.

but weak relationship indicates that melt waters from cryospheric loss may compensate for low flow, and even mitigate water shortage risks. Also, the compensating effect from cryosphere is much stronger in the MYZR ($r = 0.47$, $p > 0.05$), and together with climate contributions, contributes to the increasing WY trend (Figure 4). Different from other regions, however, the HYZR basin shows a significantly positive relationship between cryospheric contributions and total WY deviations ($r = 0.76$, $p < 0.05$), indicating that cryosphere instead of climate leads to the downward trend in headwaters. This signifies that in this region, cryospheric contributions have already passed a maximum supplying to river flow, due to decreased glaciers and snow under continuous warming. The is further verified by the relationship of cryospheric contributions to total WY (RC_g) with temperature (Figure S8). In the HYZR basin, WY resulting from the cryosphere continues to increase with temperature until a maximum is reached, beyond which cryospheric contribution to total WY begins to decrease. In addition, the compensating

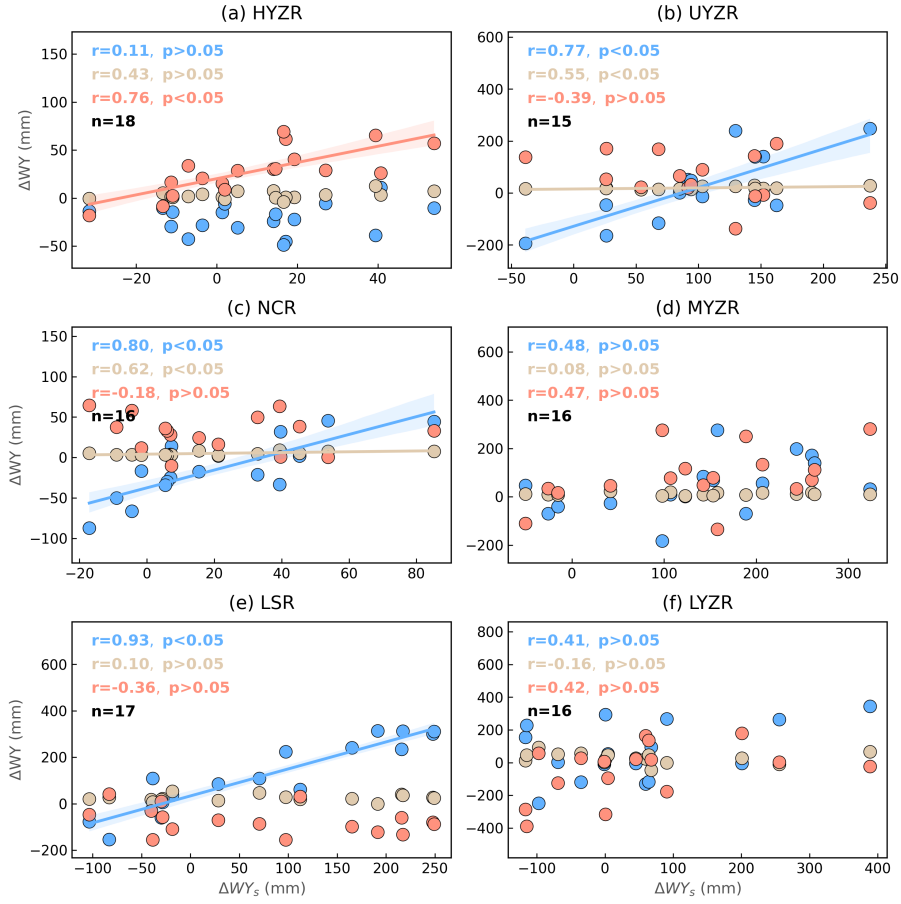

Figure 6. The correlation between time series of total water yield deviation ($\Delta WY_s(t)$, x-axis) and its components (y-axis) caused by climate ($\Delta WY_c(t)$, blue point), vegetation ($\Delta WY_v(t)$, tan point), and cryosphere ($\Delta WY_g(t)$, red point), respectively. The fitting line and its 95% confidence interval are shown only when p value < 0.05. n indicates the number of years after the TP, which is determined by the Pettitt method (See Table 1 and Figure 3c).

effect of melt waters can be seen clearly in the UYZR, MYZR and LSR basins, i.e., WY caused by cryospheric loss keeps a positive relationship with the increase of temperature, further supporting the higher correlation in these basins (Figure 6).

4 Discussion

4.1 Climate and cryosphere cause water yield regime shifts

Previous studies have indicated the increasing WY trend in the LSR (Lin et al., 2020), LYZR (Zhang et al., 2011), and UBR basins (Li et al., 2021). Here, we not only provide further evidence on the long-term trend of WY changes in the above regions,

but also conduct trend analysis in other regions that received less attention in the present. As such, the study comprehensively indicates a general increase in WY (Figure 3a) in the entire UBR basin. Further, we find that WY regime shifts occur during the late 1990s in the entire UBR basin – the magnitude in WY increases (Figure 4a), but the direction has reversed or slowed after the TP (Figure 4b). The result agrees with climate shifts (Figure S2), drought changes (Li et al., 2019b) in the UBR basin, and lake area changes in the Tibetan Plateau (Zhang et al., 2017).

Attribution analysis on WY magnitude shifts gives an emphasis on the dependency of spatial gradients of climate and cryosphere accounting for WY changes. That is, climate explains a greater increase in WY in downstream regions, while melt water is more important in upstream regions (Figure 5). This may be attributed to divergent water supply sources; Biemans et al. (2019) indicates that melt waters supply over 40% of river flow in the upper regions, but the contribution is less than 30% in the downstream in the UBR basin (Figure S9). Vegetation here does not significantly affect total river flow in the UBR (Figure 5), despite its remarkable role in seasonal runoff detected by Li et al. (2021).

Climate, especially precipitation, still control the declining WY trend after the TP in most regions (Figure 6 and S7), may become an important factor in occurrence of turning points (Figure 3c+d). This suggests the importance of precipitation and its projections on future hydrological process in mountainous watersheds (Lutz et al., 2014). Cryospheric contribution is also important for water yield regime shifts – melt waters from glaciers and snow melting can alleviate water resources shortages, mainly caused by decreased precipitation in recent years (Figure 6+S7). This finding is also supported by observed glacier runoff data (Yao et al., 2010) and several modeling studies (Lutz et al., 2014; Zhang et al., 2020; Wang et al., 2021). However, after glacier runoff reaches a maximum, defined as "peak water" (Gleick and Palaniappan, 2010), cryospheric mass loss cannot sustain the rising melt waters with atmospheric warming (e.g. the HYZR basin in Figure S8), which is in agreement with Huss and Hock (2018).

4.2 Uncertainties and limitations

This study has some limitations regarding the DMC model to partition the effects of climatic and cryospheric changes on the hydrological regime shifts in the UBR basin. The DMC method is a useful alternative statistical method to physical modeling approaches, especially in alpine river basins (e.g. UBR basin) where there is less knowledge on the complex hydrological mechanisms. While the method is still dependent on our prior understanding of hydrological responses to warming and related environmental changes, such as glaciers melting and vegetation greening. For the UBR basin, besides climate change, cryosphere (Biemans et al., 2019; Yao et al., 2019) and vegetation (Li et al., 2021, 2019a) are two major factors for hydrological changes, and the cryospheric contributions can be regarded as the deviations between total water yield and climate and vegetation contributions estimated by the DMC method. While, in some mountainous basins, human activities, such as urbanization, dam regulation and irrigation, may consume severely water resource or change seasonal runoff patterns, and thus we have to consider anthropogenic impacts into the DMC statistical model for river flow attribution. On the other hand, the DMC method applies the linear assumption between two variables, and thus it may fail to capture some nonlinear process among the interactions among water yield, vegetation and cryospheric melting in the study. Thus, with the availability of long-term in-situ observations and high-resolution remote sensing datasets in the UBR basin (Wang et al., 2022), other powerful statistical mod-

els considering nonlinear and casual structures should be applied to identify the causes of water yield changes (Runge et al., 2019).

The data used in the study may also give rise to some uncertainties for our results. The 10x10 km precipitation product used here is generated by topographical and linear corrections based on observations. As Sun and Su (2020) pointed, while, the results of the linear correction approach highly vary with the station density. For example, the increased numbers from 4 to 10 stations in the basin will decrease the mean annual precipitation by about 20 mm. Hence, the reconstruction of precipitation dataset will rely on the density of the observed stations. Besides the topographic correction, the effects of the basin size and climate seasonality should be considered in the work of precipitation reconstruction in the UBR basin due to the complex climate and environment (Sun et al., 2019). Compared with precipitation, the estimation of evaporation may be much more challenging in high mountains. Although GLEAM actual evaporation shows the good agreement with in-situ eddy covariance records (Yang et al., 2017), its model structure does not include wind speed and solar radiation, which may affect the estimation of sublimation, and thus total evaporation (Li et al., 2019c). In addition, the coarse spatial resolution with a 0.25° spatial resolution in GLEAM may be insufficient to estimate regional evaporation in the UBR basin. However, with the help of the Second Tibetan Plateau Scientific Expedition and Research, the observation networks in meteorology, cryosphere and hydrology will be built, which is expected to benefit reliable precipitation and evaporation estimation, and make developing physically-based cryosphere-hydrological modeling possible (Wang et al., 2022).

4.3 Broad Implications for mountainous water management

Understanding the hydrological regime shifts and their causes in the high mountains are especially important in managing water resources, especially balancing the co-benefits between mountains and downstream lowlands (Viviroli et al., 2011). In the study, the combined (offsetting or additive) effects from climate and cryosphere are detected (Figure 5), and further lead to either slight or substantial increases in WY in the entire UBR basin (Figure 4a). The combined effects often hinder the roles of each driver in hydrological changes (Wei et al., 2018; Zhang and Wei, 2021), which should be considered when designing water management strategies in the large transboundary river system. For example, the additive effect may be beneficial for mitigating droughts and water shortage during droughts, but it may exacerbate the flood risks due to increased precipitation and accelerated melting of the cryosphere in the future (Immerzeel et al., 2013). In addition, our results clearly show that the melt waters from glaciers might have already surpassed the "peak water" (Figure S8), and the associated hydrological changes will substantially affect future water resources management. Thus, the projections of the occurrence time of "peak water" will be important in managing mountainous water resources.

5 Conclusions

In this study, regime shifts in WY are detected during the late 1990s in the UBR basin. The WY magnitude generally increases, but its direction has reversed or slowed in recent years. Attribution analysis based on the DMC method shows that, the combined effects of climate and cryosphere are either offsetting or additive, leading to slight or substantial WY increases, while the role

of vegetation is much weaker. The declining or slowing WY trend after the TP is mainly driven by climate in most regions, while melt waters may alleviate drought and water shortage. In headwaters, however, cryospheric contributions to WY have declined due to reduced glaciers under warming. These findings suggest that the combined effects of climate and cryosphere should be considered in the sustainable development of water resources, especially involving with co-benefits in upstream and downstream regions.

Code availability. Python scripts used to extract data, analyze data, and create figures are available upon request from Hao Li (hao.liwork@ugent.be).

Data availability. Annual runoff data during 1982 and 2013 from six hydrological stations are provided by the Hydrology and Water Resources Survey Bureau of the Tibet Autonomous Region. The 10x10 km gridded daily precipitation dataset is accessed throughout https://www.tpdc.ac.cn/. The GLEAM AET is accessed from https://www.gleam.eu/. The maximum 2 m air temperature from China Meteorological Forcing Dataset is acquired via https://www.tpdc.ac.cn/. The map of land use types in 2000 is accessed from https://www.resdc.cn/.

Author contributions. HL: conceptualisation, data curation, formal analysis, methodology, writing–original draft, writing – review and editing. LL: conceptualisation, formal analysis, methodology, writing – review and editing, funding acquisition. BYS: data curation, methodology. LW: supervision, writing – review and editing. AK: validation, writing – review and editing. FZ&DFL: software, validation. XXW: visualization. WFL&XPL: Writing – review & editing. ZXX: supervision, resources.

Competing interests. The contact author has declared that neither they nor their co-authors have any competing interests.

Acknowledgements. This work was jointly supported by the National Natural Science Foundation of China (Grant No. 51961145104, 52079138, and 91647202), the 2115 Talent Development Program of China Agricultural University (00109019), and the China Scholarship Council (Grant No. 202006350051). Hao Li thanks the China Scholarship Council (CSC) for providing financial support to pursue his PhD in Belgium.

References

Biemans, H., Siderius, C., Lutz, A., Nepal, S., Ahmad, B., Hassan, T., von Bloh, W., Wijngaard, R., Wester, P., Shrestha, A., et al.: Importance of snow and glacier meltwater for agriculture on the Indo-Gangetic Plain, Nature Sustainability, 2, 594–601, 2019.

Brahney, J., Menounos, B., Wei, X., and Curtis, P. J.: Determining annual cryosphere storage contributions to streamflow using historical hydrometric records, Hydrological Processes, 31, 1590–1601, 2017.

Cuo, L., Li, N., Liu, Z., Ding, J., Liang, L., Zhang, Y., and Gong, T.: Warming and human activities induced changes in the Yarlung Tsangpo basin of the Tibetan plateau and their influences on streamflow, Journal of Hydrology: Regional Studies, 25, 100 625, 2019.

Dierauer, J. R., Whitfield, P. H., and Allen, D. M.: Climate controls on runoff and low flows in mountain catchments of Western North America, Water Resources Research, 54, 7495–7510, 2018.

Fan, H. and He, D.: Temperature and precipitation variability and its effects on streamflow in the upstream regions of the Lancang–Mekong and Nu–Salween Rivers, Journal of Hydrometeorology, 16, 2248–2263, 2015.

Fang, H., Baret, F., Plummer, S., and Schaepman-Strub, G.: An overview of global leaf area index (LAI): Methods, products, validation, and applications, Reviews of Geophysics, 57, 739–799, 2019.

Forzieri, G., Miralles, D. G., Ciais, P., Alkama, R., Ryu, Y., Duveiller, G., Zhang, K., Robertson, E., Kautz, M., Martens, B., et al.: Increased control of vegetation on global terrestrial energy fluxes, Nature Climate Change, 10, 356–362, 2020.

Gao, P., Mu, X.-M., Wang, F., and Li, R.: Changes in streamflow and sediment discharge and the response to human activities in the middle reaches of the Yellow River, Hydrology and Earth System Sciences, 15, 1–10, 2011.

Gleick, P. H. and Palaniappan, M.: Peak water limits to freshwater withdrawal and use, Proceedings of the National Academy of Sciences, 107, 11 155–11 162, 2010.

Gonsamo, A., Ciais, P., Miralles, D. G., Sitch, S., Dorigo, W., Lombardozzi, D., Friedlingstein, P., Nabel, J. E., Goll, D. S., O'Sullivan, M., et al.: Greening drylands despite warming consistent with carbon dioxide fertilization effect, Global Change Biology, 27, 3336–3349, 2021.

Goulden, M. L. and Bales, R. C.: Mountain runoff vulnerability to increased evapotranspiration with vegetation expansion, Proceedings of the National Academy of Sciences, 111, 14 071–14 075, 2014.

Hallema, D. W., Sun, G., Caldwell, P. V., Norman, S. P., Cohen, E. C., Liu, Y., Bladon, K. D., and McNulty, S. G.: Burned forests impact water supplies, Nature Communications, 9, 1–8, 2018.

He, J., Yang, K., Tang, W., Lu, H., Qin, J., Chen, Y., and Li, X.: The first high-resolution meteorological forcing dataset for land process studies over China, Scientific Data, 7, 1–11, 2020.

Huss, M. and Hock, R.: Global-scale hydrological response to future glacier mass loss, Nature Climate Change, 8, 135–140, 2018.

Immerzeel, W. W., Van Beek, L. P., and Bierkens, M. F.: Climate change will affect the Asian water towers, Science, 328, 1382–1385, 2010.

Immerzeel, W. W., Pellicciotti, F., and Bierkens, M. F. P.: Rising river flows throughout the twenty-first century in two Himalayan glacierized watersheds, Nature Geoscience, 6, 742–745, 2013.

Kang, S., Xu, Y., You, Q., Flügel, W.-A., Pepin, N., and Yao, T.: Review of climate and cryospheric change in the Tibetan Plateau, Environmental Research Letters, 5, 015 101, 2010.

Kendall, M. G.: A new measure of rank correlation, Biometrika, 30, 81–93, 1938.

Li, D., Li, Z., Zhou, Y., and Lu, X.: Substantial increases in the water and sediment fluxes in the headwater region of the Tibetan Plateau in response to global warming, Geophysical Research Letters, 47, e2020GL087 745, 2020.

Li, H., Liu, L., Liu, X., Li, X., and Xu, Z.: Greening implication inferred from vegetation dynamics interacted with climate change and human activities over the Southeast Qinghai–Tibet Plateau, Remote Sensing, 11, 2421, 2019a.

Li, H., Liu, L., Shan, B., Xu, Z., Niu, Q., Cheng, L., Liu, X., and Xu, Z.: Spatiotemporal variation of drought and associated multi-scale response to climate change over the Yarlung Zangbo River Basin of Qinghai–Tibet Plateau, China, Remote Sensing, 11, 1596, 2019b.

Li, H., Liu, L., Koppa, A., Shan, B., Liu, X., Li, X., Niu, Q., Cheng, L., and Miralles, D.: Vegetation greening concurs with increases in dry season water yield over the Upper Brahmaputra River basin, Journal of Hydrology, 603, 126–981, 2021.

Li, J., Liu, D., Wang, T., Li, Y., Wang, S., Yang, Y., Wang, X., Guo, H., Peng, S., Ding, J., et al.: Grassland restoration reduces water yield in the headstream region of Yangtze River, Scientific Reports, 7, 1–9, 2017.

Li, X., Long, D., Han, Z., Scanlon, B. R., Sun, Z., Han, P., and Hou, A.: Evapotranspiration estimation for Tibetan Plateau headwaters using conjoint terrestrial and atmospheric water balances and multisource remote sensing, Water Resources Research, 55, 8608–8630, 2019c.

Lin, L., Gao, M., Liu, J., Wang, J., Wang, S., Chen, X., and Liu, H.: Understanding the effects of climate warming on streamflow and active groundwater storage in an alpine catchment: the upper Lhasa River, Hydrology and Earth System Sciences, 24, 1145–1157, 2020.

Lutz, A., Immerzeel, W., Shrestha, A., and Bierkens, M.: Consistent increase in High Asia's runoff due to increasing glacier melt and precipitation, Nature Climate Change, 4, 587–592, 2014.

Mann, H. B.: Nonparametric tests against trend, Econometrica: Journal of the Econometric Society, pp. 245–259, 1945.

Martens, B., Miralles, D. G., Lievens, H., Van Der Schalie, R., De Jeu, R. A., Fernández-Prieto, D., Beck, H. E., Dorigo, W. A., and Verhoest, N. E.: GLEAM v3: Satellite-based land evaporation and root-zone soil moisture, Geoscientific Model Development, 10, 1903–1925, 2017.

Pellicciotti, F., Buergi, C., Immerzeel, W. W., Konz, M., and Shrestha, A. B.: Challenges and uncertainties in hydrological modeling of remote Hindu Kush–Karakoram–Himalayan (HKH) basins: suggestions for calibration strategies, Mountain Research and Development, 32, 39–50, 2012.

Pettitt, A. N.: A non-parametric approach to the change-point problem, Journal of the Royal Statistical Society: Series C (Applied Statistics), 28, 126–135, 1979.

Runge, J., Bathiany, S., Bollt, E., Camps-Valls, G., Coumou, D., Deyle, E., Glymour, C., Kretschmer, M., Mahecha, M. D., Muñoz-Marí, J., et al.: Inferring causation from time series in Earth system sciences, Nature communications, 10, 1–13, 2019.

Sang, Y., Singh, V. P., Gong, T., Xu, K., Sun, F., Liu, C., Liu, W., and Chen, R.: Precipitation variability and response to changing climatic condition in the Yarlung Tsangpo River basin, China, Journal of Geophysical Research: Atmospheres, 121, 8820–8831, 2016.

Song, C., Wang, G., Sun, X., and Hu, Z.: River runoff components change variably and respond differently to climate change in the Eurasian Arctic and Qinghai-Tibet Plateau permafrost regions, Journal of Hydrology, 601, 126 653, 2021.

Sun, H. and Su, F.: Precipitation correction and reconstruction for streamflow simulation based on 262 rain gauges in the upper Brahmaputra of southern Tibetan Plateau, Journal of Hydrology, 590, 125 484, 2020.

Sun, H., Su, F., Huang, J., Yao, T., Luo, Y., and Chen, D.: Contrasting precipitation gradient characteristics between westerlies and monsoon dominated upstream river basins in the Third Pole, Chinese Science Bulletin, 65, 91–104, 2019.

Tang, Q., Lan, C., Su, F., Liu, X., Sun, H., Ding, J., Wang, L., Leng, G., Zhang, Y., Sang, Y., et al.: Streamflow change on the Qinghai-Tibet Plateau and its impacts, Chinese Science Bulletin, 64, 2807–2821, 2019.

Viviroli, D., Archer, D. R., Buytaert, W., Fowler, H. J., Greenwood, G. B., Hamlet, A. F., Huang, Y., Koboltschnig, G., Litaor, M., López-Moreno, J. I., et al.: Climate change and mountain water resources: overview and recommendations for research, management and policy, Hydrology and Earth System Sciences, 15, 471–504, 2011.

Wang, L., Yao, T., Chai, C., Cuo, L., Su, F., Zhang, F., Yao, Z., Zhang, Y., Li, X., Qi, J., et al.: TP-River: Monitoring and quantifying total river runoff from the Third Pole, Bulletin of the American Meteorological Society, 102, E948–E965, 2021.

Wang, L., Cuo, L., Luo, D., Su, F., Ye, Q., Yao, T., Zhou, J., Li, X., Li, N., Sun, H., et al.: Observing multi-sphere hydrological changes in the largest river basin of the Tibetan Plateau, Bulletin of the American Meteorological Society, 2022.

Wei, X. and Zhang, M.: Quantifying streamflow change caused by forest disturbance at a large spatial scale: A single watershed study, Water Resources Research, 46, 2010.

Wei, X., Li, Q., Zhang, M., Giles-Hansen, K., Liu, W., Fan, H., Wang, Y., Zhou, G., Piao, S., and Liu, S.: Vegetation cover—another dominant factor in determining global water resources in forested regions, Global Change Biology, 24, 786–795, 2018.

Yang, X., Yong, B., Ren, L., Zhang, Y., and Long, D.: Multi-scale validation of GLEAM evapotranspiration products over China via ChinaFLUX ET measurements, International Journal of Remote Sensing, 38, 5688–5709, 2017.

Yao, T., Li, Z., Yang, W., Guo, X., Zhu, L., Kang, S., Wu, Y., and Yu, W.: Glacial distribution and mass balance in the Yarlung Zangbo River and its influence on lakes, Chinese Science Bulletin, 55, 2072–2078, 2010.

Yao, T., Xue, Y., Chen, D., Chen, F., Thompson, L., Cui, P., Koike, T., Lau, W. K.-M., Lettenmaier, D., Mosbrugger, V., et al.: Recent third pole's rapid warming accompanies cryospheric melt and water cycle intensification and interactions between monsoon and environment: Multidisciplinary approach with observations, modeling, and analysis, Bulletin of the American Meteorological Society, 100, 423–444, 2019.

Zhang, G., Yao, T., Piao, S., Bolch, T., Xie, H., Chen, D., Gao, Y., O'Reilly, C. M., Shum, C. K., Yang, K., Yi, S., Lei, Y., Wang, W., He, Y., Shang, K., Yang, X., and Zhang, H.: Extensive and drastically different alpine lake changes on Asia's high plateaus during the past four decades, Geophysical Research Letters, 44, 252–260, 2017.

Zhang, L., Nan, Z., Wang, W., Ren, D., Zhao, Y., and Wu, X.: Separating climate change and human contributions to variations in streamflow and its components using eight time-trend methods, Hydrological Processes, 33, 383–394, 2019.

Zhang, M. and Wei, X.: Deforestation, forestation, and water supply, Science, 371, 990–991, 2021.

Zhang, M., Ren, Q., Wei, X., Wang, J., Yang, X., and Jiang, Z.: Climate change, glacier melting and streamflow in the Niyang River Basin, Southeast Tibet, China, Ecohydrology, 4, 288–298, 2011.

Zhang, Y., yu Xu, C., Hao, Z., Zhang, L., Ju, Q., and Lai, X.: Variation of Melt Water and Rainfall Runoff and Their Impacts on Streamflow Changes during Recent Decades in Two Tibetan Plateau Basins, Water, 12, 3112, 2020.

Zhou, X., Zhang, Y., Beck, H. E., and Yang, Y.: Divergent negative spring vegetation and summer runoff patterns and their driving mechanisms in natural ecosystems of northern latitudes, Journal of Hydrology, 592, 125 848, 2021.

Zhu, Z., Bi, J., Pan, Y., Ganguly, S., Anav, A., Xu, L., Samanta, A., Piao, S., Nemani, R. R., and Myneni, R. B.: Global data sets of vegetation leaf area index (LAI) 3g and fraction of photosynthetically active radiation (FPAR) 3g derived from global inventory modeling and mapping studies (GIMMS) normalized difference vegetation index (NDVI3g) for the period 1981 to 2011, Remote Sensing, 5, 927–948, 2013.